

Paper No. 1-1

PREPRINT



International association for shell structures

PACIFIC SYMPOSIUM ON HYDROMECHANICALLY LOADED SHELLS - Part I
Honolulu, Hawaii, U.S.A.

October 10-15, 1971

THE INFLUENCE OF A HIGH VELOCITY FLUID ENVIRONMENT
ON THE STATIC AND DYNAMIC STABILITY OF THIN CYLINDRICAL
SHELL STRUCTURES

Walter Horn, Graduate Student
Aerospace and Engineering Mechanics Department
The University of Texas at Austin

Gerald Barr, Staff Member
Dynamics Analysis Research Division
Sandia Laboratories, Albuquerque, New Mexico

Ronald Stearman, Associate Professor
Aerospace and Engineering Mechanics Department
The University of Texas at Austin

Reproduced From
Best Available Copy

19990817 023

UNIVERSITY OF HAWAII

Center for Engineering Research
2565 The Mall-Honolulu, Hawaii 96822

UNCLASSIFIED

FBR

5023

Security Classification

DOCUMENT CONTROL DATA - R & D

(Security classification of title, body of abstract and indexing annotation must be entered when the overall report is classified)

1. ORIGINATING ACTIVITY (Corporate author) University of Texas Dept. of Aerospace Engr. and Engr. Mechanics Austin, Texas 78712	2a. REPORT SECURITY CLASSIFICATION UNCLASSIFIED
	2b. GROUP

3. REPORT TITLE THE INFLUENCE OF A HIGH VELOCITY FLUID ENVIRONMENT ON THE STATIC AND DYNAMIC STABILITY OF THIN CYLINDRICAL SHELL STRUCTURES

4. DESCRIPTIVE NOTES (Type of report and inclusive dates)

Preprint International Association for Shell Structures

5. AUTHOR(S) (First name, middle initial, last name)

Walter J. Horn, Gerald W. Barr, Ronald O. Stearman

6. REPORT DATE October 10-15, 1971	7a. TOTAL NO. OF PAGES 24	7b. NO. OF REFS 17
---------------------------------------	------------------------------	-----------------------

8a. CONTRACT OR GRANT NO. AF-AFOSR 71-1998	9a. ORIGINATOR'S REPORT NUMBER(S)
---	-----------------------------------

b. PROJECT NO. 71-0209

c. 9782-01

d. 681307

9b. OTHER REPORT NO(S) (Any other numbers that may be assigned this report)

10. DISTRIBUTION STATEMENT

This document has bee approved for public release and sale; its distribution is unlimited

11. SUPPLEMENTARY NOTES TECH, OTHER	12. SPONSORING MILITARY ACTIVITY Air Force Office of Scientific Research(NAM) Office of Aerospace Research USAF Arlington, Virginia 22209
--	--

13. ABSTRACT

A combined theoretical and experimental research program has been carried out to investigate the stability characteristics of thin-walled circular cylindrical shell structures exposed to a high velocity fluid dynamic (aerodynamic)environment. As a result of this study, several basic observations were made concerning the degree of sophistication required in the analytical modeling of this problem. The present study shows that a supersonic fluid dynamic environment can significantly complicate the dynamic stability characteristics of thin cylindrical shell structures while introducing no significant complications to its static stability features.

RETURN TO: AEROSPACE STRUCTURES
INFORMATION AND ANALYSIS CENTER
AFFDL/FBR
WPAFB, OHIO 45433

DD FORM 1 NOV 65 1473

UNCLASSIFIED

Security Classification

THE INFLUENCE OF A HIGH VELOCITY FLUID ENVIRONMENT ON THE STATIC AND
DYNAMIC STABILITY OF THIN CYLINDRICAL SHELL STRUCTURES

Walter Horn
Graduate Student
Aerospace and Engineering Mechanics Department
The University of Texas at Austin
Austin, Texas, U.S.A.

Gerald Barr
Staff Member
Dynamics Analysis Research Division
Sandia Laboratories
Albuquerque, New Mexico, U.S.A.

Ronald Stearman
Associate Professor
Aerospace and Engineering Mechanics Department
The University of Texas at Austin
Austin, Texas, U.S.A.

ABSTRACT

A combined theoretical and experimental research program has been carried out to investigate the stability characteristics of thin-walled circular cylindrical shell structures exposed to a high velocity fluid dynamic (aerodynamic) environment. As a result of this study, several basic observations were made concerning the degree of sophistication required in the analytical modeling of this problem. It was found, for example, that small details in the description of the structural boundary conditions can strongly influence the stability of the shell. One of the more significant structural boundary condition effects was observed when the shell geometry and loading conditions were such that the edge bending disturbances were propagated well into the interior of the shell. On the other hand, when conditions were such that these edge bending disturbances were confined to a small boundary layer region near the ends of the shell no significant edge effects due to bending were noticed on the overall shell stability. Small initial deviations of the shell's surface from its idealized shape were also shown to drastically reduce its resistance to panel flutter, a dynamic instability, even though the deviations were only on the order of one shell thickness or less. Panel flutter instabilities in the presence of a laminar fluid boundary layer profile were found to be much less destructive to the shell than those originating in the presence of a turbulent profile. Furthermore, the laminar profile was also found to induce panel flutter at much lower levels of free stream energy. The highly divergent panel flutter, occurring in the presence of a turbulent profile, appeared to have a characteristic wavelength that was small compared to the radius and length of the shell. In contrast, panel flutter, occurring in the presence of a laminar profile, had a characteristic wavelength that was on the order of the radius or length of the shell. The experimentally determined panel flutter boundaries were also found to be in poor agreement with all existing theoretical predictions. At supersonic Mach numbers no significant air stream influence was noticed on the shell buckling loads. The wealth of available still air buckling data can consequently be employed to determine the buckling loads of cylindrical shells exposed to a supersonic air stream. Although most of the study was conducted on the isotropic cylindrical shell, analyses have been carried out illustrating how these results could be extended to certain types of ring and longeron stiffened cylindrical shells. When the rings and longerons divide the shell surface into identical panel elements the analyses can be reduced in a rigorous manner to that of an equivalent panel element of the system due to the circulant form of the equations of motion. This reduction procedure allows for all types of interelement (panel) coupling and is subject to the sole restriction that the dynamic phenomena be satisfactorily described by linear theory. The present study shows that a supersonic fluid dynamic environment can significantly complicate the dynamic stability characteristics of thin cylindrical shell structures while introducing no significant complications to its static stability features.

INTRODUCTION

This research embraces a combined experimental and analytical program to investigate the stability characteristics of thin-walled cylindrical shell structures exposed to a high velocity fluid environment. It includes the basic evaluation of the past and currently employed analytical modeling of the problem and suggests areas where the modeling needs further refinements. The general problem becomes one of practical consideration in the design of skin panels on space shuttle vehicles, reusable launch boosters, and high performance supersonic aircraft. Although preliminary design criteria are evolving for flat panel elements, very little design information is currently available for thin-walled shell-type structures. Further research is necessary to obtain a better understanding of the stability and also the response characteristics of thin shell structures subjected to a high velocity fluid environment which may include aerodynamic noise, boundary layer turbulence, and buffeting conditions or large scale turbulence. The present investigation is concerned only with the question as to how the stability characteristics of such structures are influenced by a high velocity external flow environment parallel to the shell axis.

The experimental phase of the research was carried out in the AEDC propulsion wind tunnel facility of the Arnold Engineering Development Center over the Mach number range 1.2 to 3.5. Fourteen different cylindrical shell configurations were studied under different internal stress levels and supersonic flow conditions. All of the shells had a common length to radius ratio of two and radius to thickness ratios from 2000 to 4000. The experimental data reduction and analytical portion of the study was carried out on the University of Texas CDC 6600 digital computer employing a FORTRAN IV computer program.

As a result of the theoretical studies several observations were made concerning the degree of sophistication required in the analytical modeling of the problem. It was found, for example, that small changes in the description of the structural boundary conditions can strongly influence the stability characteristics of the shell. One of the more significant structural boundary condition effects was observed for shells with small to moderate radius to thickness ratios preloaded under combined internal pressure and axial compressive end loads. On the other hand, when the combined geometry and loading conditions on the shell were such that they caused the shell to respond more like a membrane, the induced bending disturbances from the edge constraints were confined to a small boundary layer region near the ends of the shell and no significant edge effects due to bending were noticed on the overall shell stability. Small deviations of the shell's surface from its idealized shape were also shown to drastically reduce its resistance to panel flutter, a dynamic instability of the shell, even though the deviations were only on the order of one shell thickness or less. Even the best manufacturing methods admit this magnitude of imperfection in the fabricated shell geometries.

During the wind tunnel experiments, panel flutter instabilities in the presence of a laminar boundary layer profile were found to be much less destructive to the shell than those originating in the presence of a turbulent profile. On the other hand, the laminar or nearly laminar boundary layer profile will induce a limited amplitude panel flutter at much lower levels of free stream energy than will a turbulent profile. When panel flutter does occur in the presence of a turbulent profile, however, it was always found to be catastrophic.

The visible form of the flutter mode for the highly divergent panel flutter instability appeared to have a characteristic wavelength that was small compared to the radius and length of the shell. For the more mild limited amplitude flutter, however, this characteristic wavelength appeared to be on the order of the radius and length of the shell. The experimentally determined flutter boundaries were found to be in poor agreement, however, with the existing theoretical predictions employing both short wavelength and long wavelength approximations for the flutter mode. A comparison was also made with two traveling wave analyses for an infinite length cylindrical shell with the highly divergent flutter. This comparison was justified on the basis that the characteristic lengths of the initial unstable wave forms were small compared with the shell radius and length. The flutter boundaries predicted by this analysis occurred at a much lower level of free stream energy than the experimental boundaries. All of the theoretical predictions concerning panel flutter were thus found to be in poor agreement with the experimental observations.

Both experimental and analytical results from this investigation demonstrate that the still-air buckling characteristics of thin cylindrical shells were not significantly influenced by the supersonic air stream. The wealth of available still-air buckling data can consequently be employed to determine the buckling loads of cylindrical shells exposed to a supersonic flow field.

Although most of the analytical studies were conducted on the isotropic cylindrical shell, analyses have been carried out illustrating how these results could be extended to certain types of ring and longeron stiffened cylindrical shells. When the rings and longerons divide the shell surface into identical panel elements the analysis can be reduced in a rigorous manner to that of an equivalent panel element of the system due to the circulant form of the equations of motion. This reduction procedure allows for all types of interelement (panel) coupling and is subject to the sole restriction that the dynamic phenomena be satisfactorily described by linear theory.

The influence of a high velocity fluid environment on the stability features of thin cylindrical shell structures involves many parameters which significantly complicate the problem. The basic development and evaluation of suitable methods of analysis for this problem must, by necessity, involve both theoretical and experimental investigations. This approach has been followed in the present program. The analytical definition and modeling of the problem are presented first along with the theoretical results obtained from the problem solutions. Experimental observations made during this study are then presented. Finally, evaluation of existing theoretical models of this problem are made based upon the available experimental data, and recommended refinements for future analytical modeling are presented.

THEORETICAL STUDY

Due to the expense and difficulty involved in conducting an experimental study of this problem the shell aeroelastic stability was investigated initially from an analytical point of view to gain further insight into the parameters that may significantly influence the experiment. The model under study, flow conditions, and static loading conditions are shown in Fig. 1. This model represents a thin-walled, finite length, isotropic cylindrical shell structure with a large radius to thickness ratio and small initial deviations of its median surface from that of a perfect circular cylindrical shell. The initial imperfections are axisymmetric having a harmonic wave form in the axial direction. The outer surface of the shell is exposed to a supersonic potential flow parallel to the shell axis. The static loading on the shell consists of an axially compressive end loading, an internal pressure loading, and a hydrostatic pressure loading on the outer surface due to the flow field. This model was thought to include most of the significant parameters that influence the shell's aeroelastic stability. That is, the influence of such different parameters as initial geometric imperfections, structural boundary conditions, different potential flow approximations, and prestress levels could all be readily investigated with this model.

Problem Formulation

The problem formulation is separated into two major categories as illustrated in Fig. 2 [3]. The first formulation is based on a perfect circular cylindrical shell, whereas the second formulation centers around a shell with axisymmetric initial imperfections of harmonic wave form. Both formulations contain the so-called classical analysis, PATHS No. 1 and No. 3, and a nonclassical analysis, PATHS No. 2 and No. 4, as special cases. In the classical analysis, a kinetic stability solution is considered by investigating the

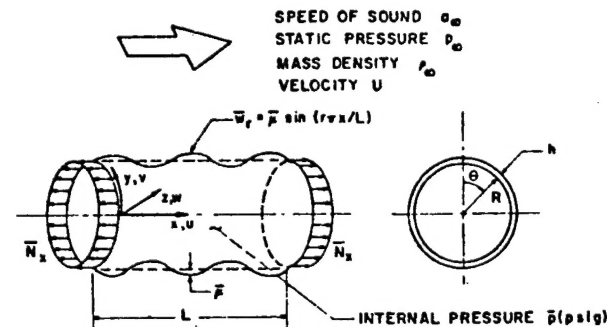


Fig. 1
Shell Geometry and Flow Conditions

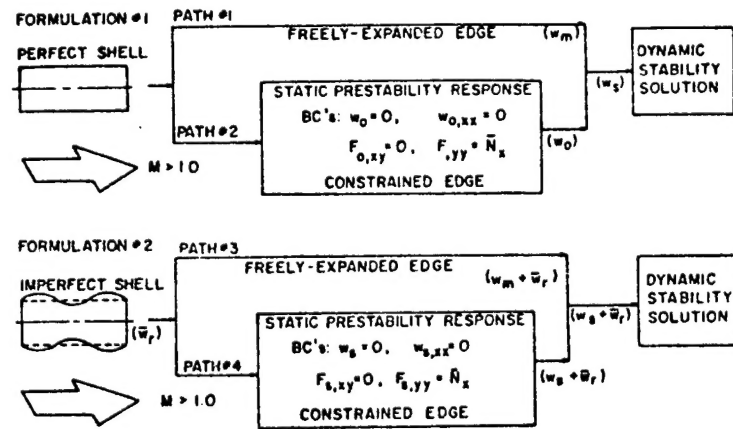


Fig. 2
Formulation of Aeroelastic Stability Problem

behavior in time of small displacement perturbations with respect to the middle surface of the original shell geometry which is either a perfect shell, PATH No. 1, or an imperfect shell, PATH No. 3. Any change in the shell static equilibrium shape due to axially compressive end loading, internal pressure loading, or fluid dynamic loading prior to the instability is ignored. The stress state in the shell is determined from membrane theory and the static or dynamic stability of the shell is investigated about its originally specified geometric shape. In contrast, the nonclassical analysis determines the statically deformed middle surface (predeformation shape) of the shell due to initial loading conditions prior to an instability and then investigates the stability of the shell about this newly calculated equilibrium surface employing a kinetic stability approach. In essence, the nonclassical approach attempts to more realistically model the actual structural boundary conditions in the problem. An additional formulation of the problem was also carried out employing the so-called "freely supported" boundary conditions in contrast to those shown in Fig. 2. These basic formulations lead to refinements in the structural modeling of the problem in at least two areas. They can be classified as a predeformation effect and a direct structural boundary condition effect. The latter results from specifying different structural boundary conditions on the ends of the shell whereas the former results from an interaction of the initial prestress, in an otherwise perfect or imperfect shell, with the structural boundary constraints.

A set of nonlinear Donnell type shell equations coupled with a linear potential flow theory was employed to describe the motion of the shell and the radial surface pressure loading respectively in the presence of a supersonic flow field. Geometric nonlinearities along with the initial imperfections are introduced into the shell theory through the strain-displacement relations. In-plane inertia of the shell has been neglected in the equations of motion due to the anticipated predominately radial motion of the shell during an instability. The governing equations of motion of a cylindrical shell with small initial deviations of the median surface are written in terms of the radial displacement w , and the total stress function F , as

$$\frac{1}{Eh} \nabla^4 F = w_{xy}^2 - w_{xx} w_{yy} + \frac{1}{R} w_{xx} - \bar{w}_{r,xx} w_{yy} - \bar{w}_{r,yy} w_{xx} + 2\bar{w}_{r,xy} w_{xy} \quad (1)$$

$$D \nabla^4 w + \frac{1}{R} F_{,xx} - F_{,yy} (w_{xx} + \bar{w}_{r,xx}) - F_{,xx} (w_{yy} + \bar{w}_{r,yy}) + 2F_{,xy} (w_{xy} + \bar{w}_{r,xy}) = p(x,y,t) \quad (2)$$

where the commas denote partial differentiation. The associated boundary conditions of a shell with simply supported "zero tangential shear stress" edges at $x=0, L$ are

$$\begin{aligned} w(x,y,t) &= w(x,y,t)_{,xx} = F(x,y,t)_{,xy} = 0 \\ F(x,y,t)_{,yy} &= \bar{N}_x \end{aligned} \quad (3)$$

while the classical "freely supported" boundary conditions are

$$u(x,y,t)_{,x} = v(x,y,t) = w(x,y,t) = w(x,y,t)_{,xx} = 0 \quad (4)$$

The surface loading on the shell may be defined as

$$p(x,y,t) = \bar{p} - \rho_s h \hat{w}_{,tt} + p_a \quad (5)$$

where the first term represents the static pressure differential across the skin of the shell and the second term is the inertial loading resulting from the motion of the shell surface. The radial aerodynamic pressure is obtained from limiting cases of the exact supersonic potential flow solution over a finite length shell with a harmonically oscillating surface. The approximations are valid for the so-called long and short wavelength modes of shell instability. They are obtained from the solution of the following boundary value problem.

$$\begin{aligned}
\frac{1}{r^2} \frac{\partial^2 \phi}{\partial \theta^2} + \frac{\partial^2 \phi}{\partial r^2} + \frac{1}{r} \frac{\partial \phi}{\partial r} - \beta^2 \frac{\partial^2 \phi}{\partial x^2} &= 2 \frac{M}{a} \frac{\partial^2 \phi}{\partial x \partial t} + \frac{1}{a^2} \frac{\partial^2 \phi}{\partial t^2} \\
\left. \frac{\partial \phi}{\partial r} \right|_{r=R} &= \frac{V_R}{U} = \frac{\partial w}{\partial x} + \frac{1}{U} \frac{\partial w}{\partial t} = w(x, \theta, t) \\
\phi &= 0 \quad x \leq 0 \\
\phi &\rightarrow 0 \quad r \rightarrow \infty \quad x > 0 \\
C_p &= -2 \left(\frac{\partial \phi}{\partial x} + \frac{1}{U} \frac{\partial \phi}{\partial t} \right)
\end{aligned} \tag{6}$$

where ϕ is a perturbation velocity potential induced by the shell radial deformation w . The total velocity potential being $\Phi = U(x+\phi)$. In addition, r , θ , and x are polar coordinates as indicated in Fig. 1 while U is the magnitude of the free stream velocity, M the free stream Mach number, and a the speed of sound in the undisturbed flow. The pressure coefficient C_p is defined in terms of the perturbation pressure, p , and the free stream static pressure, p_∞ , and the dynamic pressure, q_∞ , as

$$C_p = \frac{p - p_\infty}{q_\infty}$$

The systems of Eqs. (1), (2), (3) or (4), (5), and (6) are solved subject to the restriction of simple harmonic motion and the stability analysis reduced to the solution of a complex eigenvalue problem. More specifically, the combination of physical parameters (such as flow velocity, fluid density, shell geometry, etc.) that lead to one or more real valued eigenvalues represents the desired solutions of interest.

Method of Solution

A complete consistent solution to the stability problem is accomplished in two steps. The first step determines the prestability deformation of the middle surface due to the application of initial preloads and radial pressure from the air stream. This deformation is determined in closed form from a set of steady-state response equations obtained by separating Eqs. (1) and (2) into their static and dynamic components after making the following substitutions

$$\begin{aligned}
w(x, y, t) &= w_s(x) + w^0(x, y, t) \\
F(x, y, t) &= F_s(x, y) + F^0(x, y, t) \\
p(x, y, t) &= p_s(x) + p^0(x, y, t)
\end{aligned} \tag{7}$$

This is possible because of the axisymmetric property of the initial imperfections, the surface loading, and the resulting prestability deformations. A set of equations governing the static prestability deformations (subscript s) is obtained by virtue of the equilibrium state existing prior to the instability. A second set of linearized equations in terms of the dynamic components (superscript 0) govern the dynamic or static stability of the shell about its deformed middle surface. The two systems of equations are coupled through the induced static deformation and stress terms.

The deformed middle surface of the shell (predeformation state) is determined from the following set of steady state response equations

$$Dw_{s,xxxx} + (1/R)F_{s,xx} - F_{s,yy}w_{s,xx} = p_s(x) + F_{s,yy}\bar{w}_{r,xx} \tag{8}$$

and

$$(1/Eh)\nabla^4 F_s = (1/R)w_{s,xx} \tag{9}$$

and the associated boundary conditions at $x=0, L$ of

$$w_s(x) = w_s(x)_{,xx} = F_s(x,y)_{,xy} = 0; \quad F_s(x,y)_{,yy} = \bar{N}_x \quad (10)$$

or in the case of freely-supported edges

$$u_s(x)_{,x} = v_s(x) = w_s(x) = w_s(x)_{,xx} = 0 \quad (11)$$

The initial geometric imperfection is defined as

$$\bar{w}_I = \bar{\mu} \sin(r\pi x/L) \quad (12)$$

The general analytic solution is obtained by solving Eq. (9) for the appropriate derivatives of the stress function which reduce Eq. (8) to the form of an ordinary fourth order linear inhomogeneous differential equation with constant coefficients. This is then readily solved in closed form by standard methods. After this first step of the solution is completed, the second procedure involves obtaining nontrivial solutions to the following linearized dynamic set of linear partial differential equations possessing variable coefficients

$$D\nabla^4 w^0 + \frac{1}{R} F^0_{,xx} - F^0_{s,yy} w^0_{,xx} - F^0_{s,xy} w^0_{,yy} - F^0_{,yy} (w^0_s + \bar{w}^0_I) + 2F^0_{s,xy} w^0_{,xy} = p^0(x,y,t) \quad (13)$$

and

$$\frac{1}{Eh} \nabla^4 F^0 = \frac{1}{R} w^0_{,xx} - (w^0_s + \bar{w}^0_I) w^0_{,yy} \quad (14)$$

The primes denote ordinary differentiation with respect to x . The associated boundary conditions are

$$w^0(x,y,t) = w^0(x,y,t)_{,xx} = F^0(x,y,t)_{,xy} = F^0(x,y,t)_{,yy} = 0 \quad (15)$$

or for the freely-supported case

$$u^0(x,y,t)_{,x} = v^0(x,y,t) = w^0(x,y,t) = w^0(x,y,t)_{,xx} = 0 \quad (16)$$

The specific form of the variable coefficients are obtained from a solution of the static response problem and the form of initial imperfection. Modal solutions of the dynamic equations are sought in the form

$$\begin{aligned} \bar{w}^0(a, \theta, \tau) &= f(a) \cos n\theta e^{ik\tau} \\ \bar{F}^0(a, \theta, \tau) &= g(a) \cos n\theta e^{ik\tau} \end{aligned} \quad (17)$$

$$\text{with: } \tau = \frac{Ut}{R} \quad k = \frac{\omega R}{U} \quad (k \text{ real}) \quad a = \frac{x}{R}$$

where the axial deformation function and axial stress function satisfying the boundary conditions are denoted by

$$\begin{aligned} f(a) &= \sum_{m=1}^N \tilde{X}_m \sin Z_m a \\ g(a) &= \sum_{m=1}^N \tilde{Y}_m \sin Z_1 a \sin Z_m a \quad Z_m = m\pi/(L/R) \end{aligned} \quad (18)$$

or for freely-supported edges by

$$\begin{aligned} f(a) &= \sum_{m=1}^N \tilde{X}_m \sin Z_m a \\ g(a) &= \sum_{m=1}^N \tilde{Y}_m \sin Z_m a \end{aligned} \quad (19)$$

Galerkin's approximate solution method was then applied simultaneously to Eqs. (13) and (14) reducing the equations to the matrix form of a nonlinear eigenvalue problem with eigenvalue k .

$$[k^2 B_0 - kB_1 - B_2] \tilde{X} = 0 \quad (20)$$

The system was then transformed to the form of an equivalent linear eigenvalue problem,

$$\det [A - kI] = 0 \quad (21)$$

Having the same eigenvalues as Eq. (20) [7].

The stability criteria employed in the analysis observes the behavior of the eigenvalue k as a function of the free stream static pressure or applied axial load. The time dependent part of the dynamic solution is of the form

$$w^0(a, \theta, r) \sim e^{ikr}$$

The onset of a dynamic instability occurs when the imaginary part of k changes sign from a positive to negative value while the real part remains finite but nonvanishing. At the critical stability boundary the shell motion becomes undamped simple harmonic. In contrast, a static instability occurs at zero frequency. The real part of k vanishes as the imaginary part of k changes sign from a positive to negative value. The latter form of instability is frequently classified as a buckling or divergence phenomena while the former represents a panel flutter instability.

In the above method of solution, the specific form of the aerodynamic pressure approximations was not mentioned and a few comments on this are in order. In keeping with the general form of solution, the perturbation velocity potential, radial displacement and down wash components were expressed as

$$\begin{aligned} \phi(x, r, \theta, t) &= \phi_n(x, r) \cos n\theta e^{i\omega t} \\ w(x, \theta, t) &= w_n(x) \cos n\theta e^{i\omega t} \\ W(x, \theta, t) &= W_n(x) \cos n\theta e^{i\omega t} \end{aligned} \quad (22)$$

Upon substituting this into Eq. (6) and applying the Laplace transformation

$$\bar{\phi}_n(p, t) = \int_0^\infty e^{-px} \phi_n(x, r) dx \quad (23)$$

To the resulting equations one obtains the following solution for the transformed perturbation velocity potential

$$\bar{\phi}_n(p, t) = R \bar{W}_n(p) \frac{K_n(qr)}{qK'_n(q)} \quad (24)$$

where

$$q^2 = \left(\frac{R\beta}{L}\right)^2 p^2 + 2M^2 i\omega \left(\frac{R}{L}\right) p - \omega^2 M^2$$

and K_n is a modified Bessel Function of the second kind. Upon inversion the velocity potential may be expressed as

$$\bar{\phi}_n(x, r, \theta, t) = R \cos n\theta e^{i\omega t} \int_0^x W_n(z) U_n(x-z) dz \quad (25)$$

Where the aerodynamic Kernel function is defined in terms of the inverse Laplace transform

$$U_n(x,r) = \frac{1}{2\pi i} \int_{c-i\infty}^{c+i\infty} e^{px} \frac{K_n(qr)}{qK'_n(q)} dq \quad (26)$$

Now this aerodynamic Kernel function for unsteady flow can be expressed in terms of the previously defined Randell functions which arise in the solution of the steady flow problem [13]. That is

$$U_n(x,r) = \left(\frac{L}{\beta R} \right) e^{-i \frac{\omega L}{R} \left(\frac{M^2}{\beta^2} \right) x} \left\{ V_n \left[\frac{L}{\beta R} x, r \right] - \frac{\omega M}{\beta} \left(\frac{L}{\beta R} \right) \int_0^x J_1 \left[\frac{\omega M}{\beta} \left(\frac{L}{\beta R} \right) u \right] V_n \left[\frac{L}{\beta R} (x^2 - u^2)^{1/2}, r \right] du \right\} \quad (27)$$

with

$$-V_n(\bar{x},r) = \frac{1}{2\pi i} \int_{a-i\infty}^{a+i\infty} \frac{e^{i\bar{x}\xi} K_n(\xi r)}{\xi K'_n(\xi)} d\xi, \quad \bar{x} = \frac{L}{\beta R} x$$

The pressure loading on the shell surface associated with the n^{th} circumferential deformation mode is then given by

$$C_p = -\frac{2}{L} \left(\frac{\partial \phi_n}{\partial x} + i \frac{\omega L}{R} \phi_n \right)_{r=1} \quad (28)$$

which after an appropriate integration by parts may be expressed as

$$C_p = \frac{2}{\beta L} \cos n\theta e^{i\omega t} \left\{ \left[\frac{\partial w_n}{\partial x} + i \frac{\omega L}{R} \left\{ 1 - \left(\frac{M^2}{\beta^2} - 1 \right) \right\} \left[w_n - \frac{L}{2\beta R} w_n \right] + \int_0^x w_n(z) e^{-i \frac{\omega L}{R} \frac{M^2}{\beta^2} (x-z)} G_n [U_n'', U_n', U_n] dz \right] \right\} \quad (29)$$

Now for short wavelength instabilities occurring at high Mach numbers the integral correction term becomes quite small and can be neglected [5,9]. This resulting piston theory expression with a first-order curvature correction term was employed to estimate the unsteady air loads on the shell in the so-called short wavelength approximations.

The long wavelength approximation is based upon the following asymptotic approximation to the aerodynamic Kernel function $U_n(x)$ [5,6,10].

$$\frac{K_n(a)}{a K'_n(a)} \approx -\frac{1}{(n^2 + a^2)^{1/2}} \quad n \neq 0, \quad |n^2 + a^2|^{3/2} \gg n^2 + 1$$

The above approximation is exact as a tends to either 0 or ∞ . That is, as the shell surface approaches a slender or planar configuration to the air stream. In the limiting case $a \rightarrow 0$ the aerodynamic Kernel function takes on the characteristic of a delta function, i.e.,

$$\frac{K_n(a)}{a K'_n(a)} \rightarrow -\frac{1}{n} \quad a \rightarrow 0$$

$$U_n(a) \rightarrow -\frac{R}{n} \delta(x)$$

and the pressure coefficient can be approximated as

$$C_p \cong \frac{2R}{n} \cos n\theta e^{i\omega t} \left[\left(\frac{\partial w_n}{\partial x} + \frac{i\omega}{U} w_n \right)_{x=0} \delta(x) + \left(\frac{\partial}{\partial x} + \frac{i\omega}{U} \right)^2 w_n(x) \right] . \quad (30)$$

The pressure singularity at the leading edge of the shell will give rise to a concentrated generalized aerodynamic force acting at this edge when it is not restrained against radial deflections. This is a consequence of applying slender body theory to a configuration possessing a discontinuity in cross section. In essence the pressure singularity need be retained only in those flutter analyses where the shell leading edge is not completely restrained against radial movement.

Slender body theory and piston theory are a plausible approximation to the aerodynamic pressures for predicting a low supersonic Mach number long wavelength instability and a high supersonic Mach number short wavelength instability, respectively. They were the two potential flow approximations employed in the present study to estimate the steady and unsteady pressure loadings on the shell surface due to the supersonic flow field.

Theoretical Results

The theoretical investigations carried out to date have looked into the influence of initial geometric imperfections, refinements in modeling structural boundary conditions, and different aerodynamic approximations on the accuracy in estimating the aeroelastic stability characteristics of thin cylindrical shell structures. Several definitive observations have resulted from the theoretical study which are detailed in the following.

a) Influence of Structural Boundary Conditions on the Shell's Aeroelastic Stability

Refinements in modeling the structural boundary conditions were carried out in two basic areas of interest. These were classified as a predeformation effect and a direct structural boundary condition effect. The latter results from specifying different structural conditions on the ends of the shell whereas the former results from an interaction of the initial prestress, in an otherwise perfect or imperfect shell, with the structural boundary constraints. That is, when predeformations are considered, stability is investigated about the deformed state of the shell instead of its freely expanded or undeformed state. This deformed state results from preloading the shell with a combined internal pressure and/or uniform axial loading in the presence of an air stream and realistic boundary constraints. The modified piston theory approximation, given by Eq. (29), with the integral term neglected, was employed to estimate the aerodynamic pressure loadings.

The basic problem under consideration here was the formulation no. 1 illustrated in Fig. 2. When predeformation effects were considered path no. 2 was followed in this problem formulation and the shell's aeroelastic stability investigated about its predeformation state. When path no. 1 was followed in the problem formulation the preloading on the shell did not change the basic shell geometry and stability was investigated about the shell's initial or undeformed state. This slight refinement in structural modeling implied by path no. 2 can have an influence on the stability characteristics of the shell as illustrated in Figs. 3 and 4. In Fig. 3 it is shown that when the combined loading and geometry were such that the predeformation effects were propagated from the ends of the shell well into its interior a 15 to 20 percent shift was observed in the flutter boundary of highly stressed shells. This predeformation influence was found to stabilize the shell. On the other

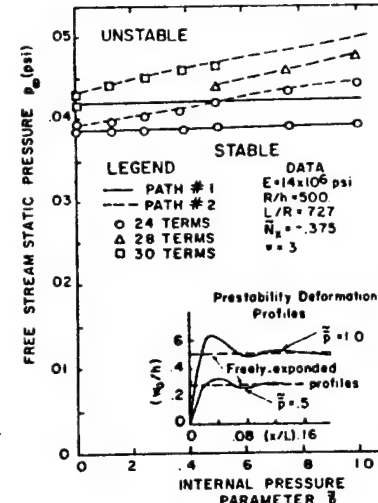


Fig. 3
Aeroelastic Stability Boundaries
for Copper Shell at Mach 5.0
and $R/h=500$

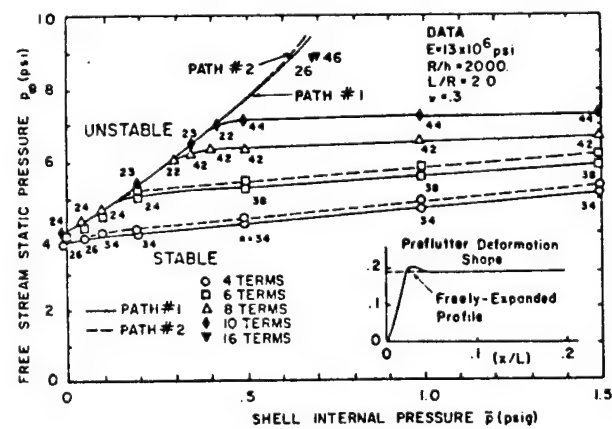


Fig. 4
Aeroelastic Stability Boundaries at $N_x=0$ Path #1
and #2 Solutions

hand, for certain shell geometries and loading conditions the predeformation influences were restricted to a small region or boundary layer adjacent to the ends of the shell and no significant influences were obtained as illustrated in Fig. 4. The influence of applying different structural boundary conditions on the ends of the shell was investigated over a range of parameters where predeformation effects were not found to be significant. Small changes in the structural description of the boundary constraints can produce significant shifts in the aeroelastic stability of the shell. This is illustrated in Fig. 5 where changes only in the in-plane boundary conditions produced significant shifts in the aeroelastic stability boundary at the higher levels of internal stress or pressurization. Although these refinements in the modeling of the structural boundary conditions did not explain the existing discrepancy between theory and the earlier experiments, information was obtained on the accuracy required in the modeling of the structural boundary conditions for a realistic analysis. In summary it was found that the correct structural modeling of the shell must include the option of employing different structural boundary conditions as well as predeformation effects.

b) Influence of Initial Geometric Imperfections on the Shell's Aeroelastic Stability

This study represented an additional structural refinement introduced in the aeroelastic modeling of cylindrical shell structures. It represents an extension of the study conducted under part (a) and was again undertaken to help clarify the reason for the large discrepancy that existed between experimental and theoretical observations on cylindrical shell panel flutter. More specifically the existing analytical models were extended to determine the influence that small initial geometric imperfections, due to fabrication techniques, have on the aeroelastic stability behavior of cylindrical shells. The modified piston theory aerodynamic approximation was again used and the basic problem under consideration here was the formulation no. 2 illustrated in Fig. 2. When the predeformation influence of part (a) is also considered, path no. 4 is followed in the problem formulation. When the predeformation effects are neglected path no. 3 represents the appropriate formulation. The present study demonstrates how an apparently better correlation between the theory and earlier experiments can be achieved when initial geometric imperfections are considered in the analysis. The nature of the imperfections were estimated from experimental measurements on fabricated shells. This apparent improved correlation with experiments is illustrated in Fig. 6, where the results of formulation no. 1 path no. 2 are compared with the results of formulation no. 2 path no. 4. It is evident that initial geometric imperfections drastically reduced the shell's ability to resist panel flutter even when the imperfection amplitudes were only on the order of one shell thickness. The results of the present analysis extended our concept concerning the correct structural modeling for studies related to the aeroelastic stability of thin cylindrical shells. In essence, the correct structural modeling of the shell must include the option of employing different structural boundary conditions, predeformation effects, as well as initial geometric imperfections that may be present in the shell surface.

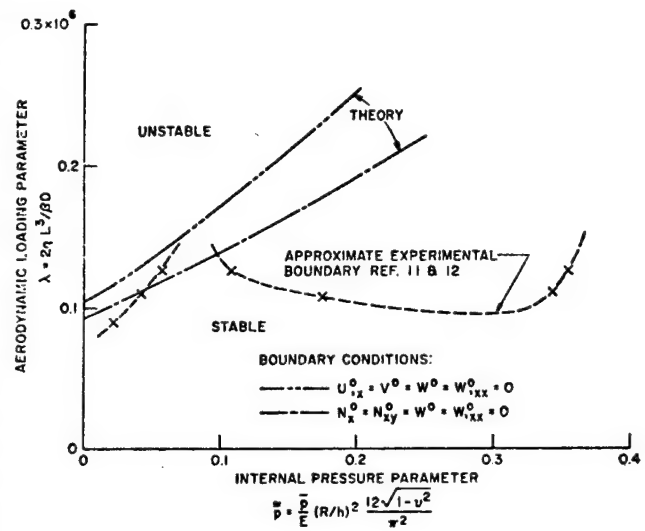


Fig. 5
Cylindrical Shell Flutter Boundaries for Two Different Structural Boundary Conditions

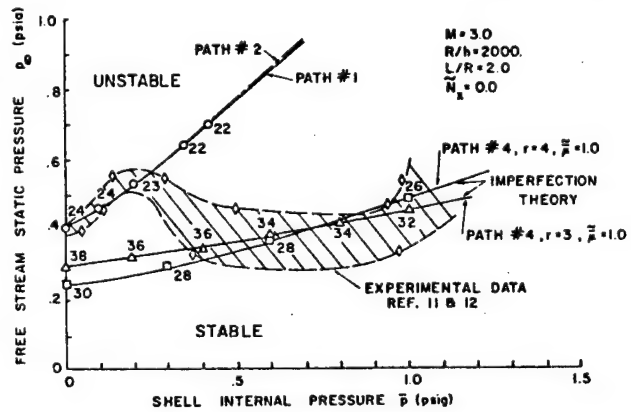


Fig. 6
Aeroelastic Stability Boundaries; Demonstration of the Effect of Initial Imperfections

It is of interest to note that a limit check on the analysis of parts (a) and (b), concerning conclusions on structural modeling, was obtained by setting the air speed equal to zero. This stability study then reduces to a classical shell buckling analysis under the influence of predeformation effects and initial geometric imperfections. This has been extensively studied in the literature and much data is readily available for comparison. The limit checks used in the present study agreed with the published results in all cases. This is illustrated in Fig. 7 [1]. This was assumed to be a sufficient verification of the analyses and computer codes developed during these studies.

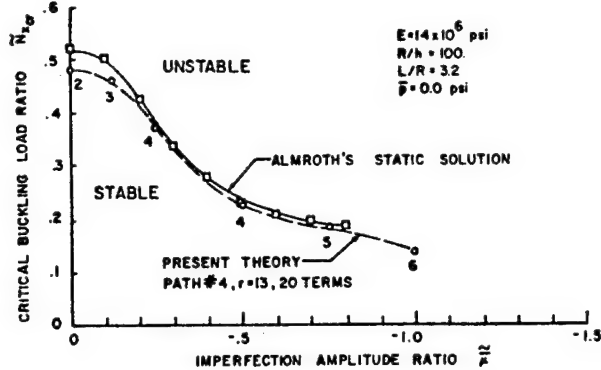


Fig. 7
Numerical Solution Limit Check

c) Influence of Supersonic Flow Field on Critical Buckling Loads of Cylindrical Shells

The structural loads imposed on many aerospace vehicles passing through the region of maximum dynamic pressure during the boost or reentry phase of a trajectory are quite severe and may result in the structure becoming aeroelastically unstable in a static mode. That is, the structure may encounter a buckling type collapse rather than a panel fluttering instability due to the combined air and inertia loads imposed upon it. Since the primary structural member is usually the thin walled cylindrical shell the problem becomes one of investigating its stability against buckling when its outer surface is exposed to a high velocity air stream. The initial preload was a combined internal pressure and axial compressive end loading and the modified piston theory approximation was again used. Primary findings in this area indicate that if the critical loading conditions occur at supersonic air speeds then the existing still air buckling data should be beneficial in the design of such shell structures. The influence of the supersonic air stream has no significant effect on the shell's ability to resist a buckling collapse. These conclusions have been confirmed on both a theoretical and experimental basis. The theoretical study employed the computer code developed under parts (a) and (b) above. Some of the theoretical data substantiating these conclusions are illustrated in Fig. 8. In this illustration three different shell internal pressures \bar{p} were examined and the corresponding stability boundaries plotted in Fig. 8. It is seen that for each shell internal pressure level, the stability behavior exhibits a similar trend as a function of the applied axial load \tilde{N}_X . As the applied axial load is increased, the ability of the shell to resist a dynamic (fluttering) type instability decreases by as much as 85-90 percent of the zero axial load case. This pronounced destabilizing trend occurs at axial loads less than 40 percent of the static still air buckling load of the shell. For axial loads above approximately 40 percent of the critical buckling load, the freestream static pressure required to cause an aeroelastic instability remains fairly constant but the critical circumferential wave number decreases until a critical axial load is reached. At this axial load, the shell diverges into a static buckled shape with a corresponding circumferential wave number equivalent to that predicted from still air buckling studies. Also, the critical divergence axial load obtained in the presence of a supersonic flow field is essentially the same as the critical buckling load predicted by the still air buckling study at corresponding shell internal pressures.

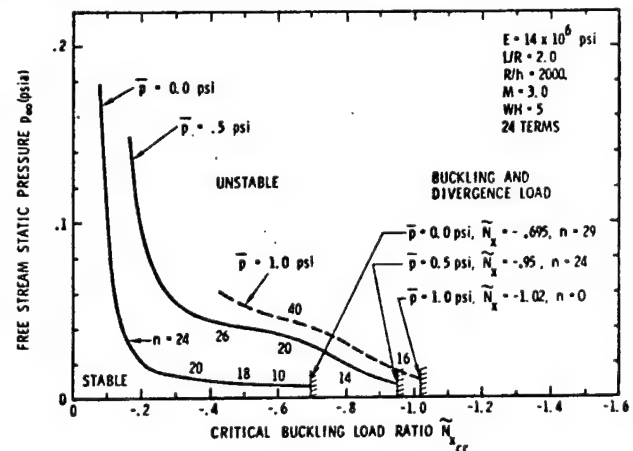


Fig. 8
Influence of Axial Compressive Loading on the
Aeroelastic Stability Boundary

It is apparent from this study that the axial load carrying capability of thin cylindrical shells is not influenced by the existence of an external supersonic flow field. This was also confirmed in the experimental study discussed below. However, this does not preclude the necessity of investigating the dynamic stability of the shell since for certain flow and stress conditions the shell may be statically stable but dynamically unstable.

d) Evaluation of Different Potential Flow Approximations

Although the aerodynamic theory most commonly employed in the reported theoretical results was the modified simple piston theory approximation, several studies have been carried out using the slender body approximation valid for long wavelength instabilities occurring at low supersonic Mach numbers [5,2]. Unfortunately, after extensive study it was found that this simple aerodynamic theory could not be expected to predict even the qualitative features of the shell dynamic instabilities that were observed experimentally. Comparisons with a good number of experimental observations indicated that slender body theory does not predict a dynamic instability (panel flutter) over the range of experimental parameters where a dynamic instability was observed. Instead slender body theory always predicted a static or divergence instability over the complete range of parameters investigated. In addition, this aerodynamic approximation indicated a significant influence of the supersonic flow field on the buckling characteristics of thin cylindrical shells that was not predicted by the modified piston theory approximation or observed experimentally. In view of this, the theory was considered to be inadequate for the present problem. The modified piston theory approximation showed reasonably close correlation with all of the earlier experimental observations on a mild limited amplitude panel flutter occurring on initially unstressed shells. It became increasingly unconservative, however, as the initial prestress in the shell was increased. In addition, it did not compare very well with a more highly divergent flutter reported for the first time in the present experimental study. Experimental observations discussed below cast further doubt on even the validity of employing the modified piston theory aerodynamic model for predicting the shell dynamic stability. In essence, all potential flow models appear to be on questionable grounds for predicting the dynamic stability characteristics of thin shell structures.

EXPERIMENTAL OBSERVATIONS

To further evaluate the accuracy of the analytical modeling in the above analysis and in the analyses carried out to date on this problem, a wind tunnel experiment was designed and conducted on 14 different cylindrical shell configurations under different internal stress levels and supersonic flow conditions. All of the shells had a common length to radius ratio of two and radius to thickness ratios from 2000 to 4000. These shell geometries were taken to be the same as those from an earlier program to facilitate a comparison of the present results with these earlier experiments [11,12]. The facilities of the 16-ft supersonic and transonic Propulsion Wind Tunnel of the Arnold Engineering Development Center was employed for the study. Full details of the wind tunnel facility are presented in [16].

Description of Flutter Model and Instrumentation

The experimental flutter model was a ogive cylinder configuration cantilevered at its base from the wind tunnel sting. The thin shells under study were isotropic circular cylindrical shells fabricated from copper by an electroforming process. The shells were bonded to two heavy copper end rings and mounted near the base of the ogive cylinder model. The electroforming process provided shell models with a high degree of uniformity in both material and geometric properties while minimizing geometric imperfections and initial fabrication stresses. In addition, extremely thin shells could be easily fabricated in this manner. A photograph of a typical test shell without end rings, and its installation in the wind tunnel is shown in Fig. 9.

Several types of instrumentation were employed on the model to observe and control the shell instabilities. Transducers were employed to monitor both static and dynamic displacements of the shell skin. Loading mechanisms were also employed that could simulate a variety of stress states in the shell by employing axial compressive end loads and/or internal pressurization. A boundary layer control slot was located in the model nose cone to artificially trip an existing laminar boundary layer profile or thicken an already fully developed turbulent profile. A variety of boundary layer rakes and static surface pressure probes were also employed to determine the nature of the local flow field over the shell. Finally, visual monitoring through high speed photography and on-line television cameras provided an additional mode of instrumentation for observing the shell instabilities. Further detailed descriptions on the model and instrumentation can be found in [8].

Observed Shell Instabilities

Two basic types of shell instabilities were observed during the course of the experiments. This included a divergence or buckling instability and a dynamic or panel fluttering instability of the shell skin in the presence of a supersonic air stream. This latter instability is similar to flag or sail flutter, while the former appears identical to the classical static buckling instability of thin shells under combined axial compressive end loading and/or internal pressure. The basic experimental procedure followed during the course of the study was to maintain wind tunnel conditions fixed and change the shell model internal stress state or boundary layer features to initiate or suppress a shell instability.

Buckling or Divergence Instability

Buckling or divergence studies were conducted to determine the influence of the supersonic air stream on the shell classical still air buckling loads, and to establish a safe shell loading limit for avoiding a divergence or static mode of shell instabilities over a range of supersonic flow conditions. Although the onset of a static divergence or buckling collapse was quite evident due to its catastrophic nature, several experimental indicators were employed to distinguish its characteristics [8]. The influence of the supersonic air stream on the classical buckling loads of thin cylindrical shells under combined axial compressive loading and internal pressurization was investigated by correlating data from at least a dozen different test conditions. These included shell buckling studies both with and without the influence of an external supersonic flow. The data are presented in Table I and on the buckling interaction curve illustrated in Fig. 10. The data represented by the shaded points in Fig. 10 were taken from still air buckling tests, while the open symbols represent wind tunnel test points. The flow conditions and radius-to-thickness ratios of each shell are indicated beside each test point. The triangular open symbols represent dynamic instabilities (panel flutter), while the remaining open symbols represent static buckling in the presence of an air stream. The data on this interaction curve indicate that no significant shift occurs in the wind tunnel buckling load points (open non-triangular symbols) when compared to their still air buckling counter parts (shaded symbols). The primary findings here indicate that if the critical loading conditions on the shell cause it to become unstable in a divergence or buckling mode at supersonic air speeds then the wealth of existing still air buckling data should be beneficial in estimating the buckling loads of such structures. The interaction design curve suggested in [17] which is

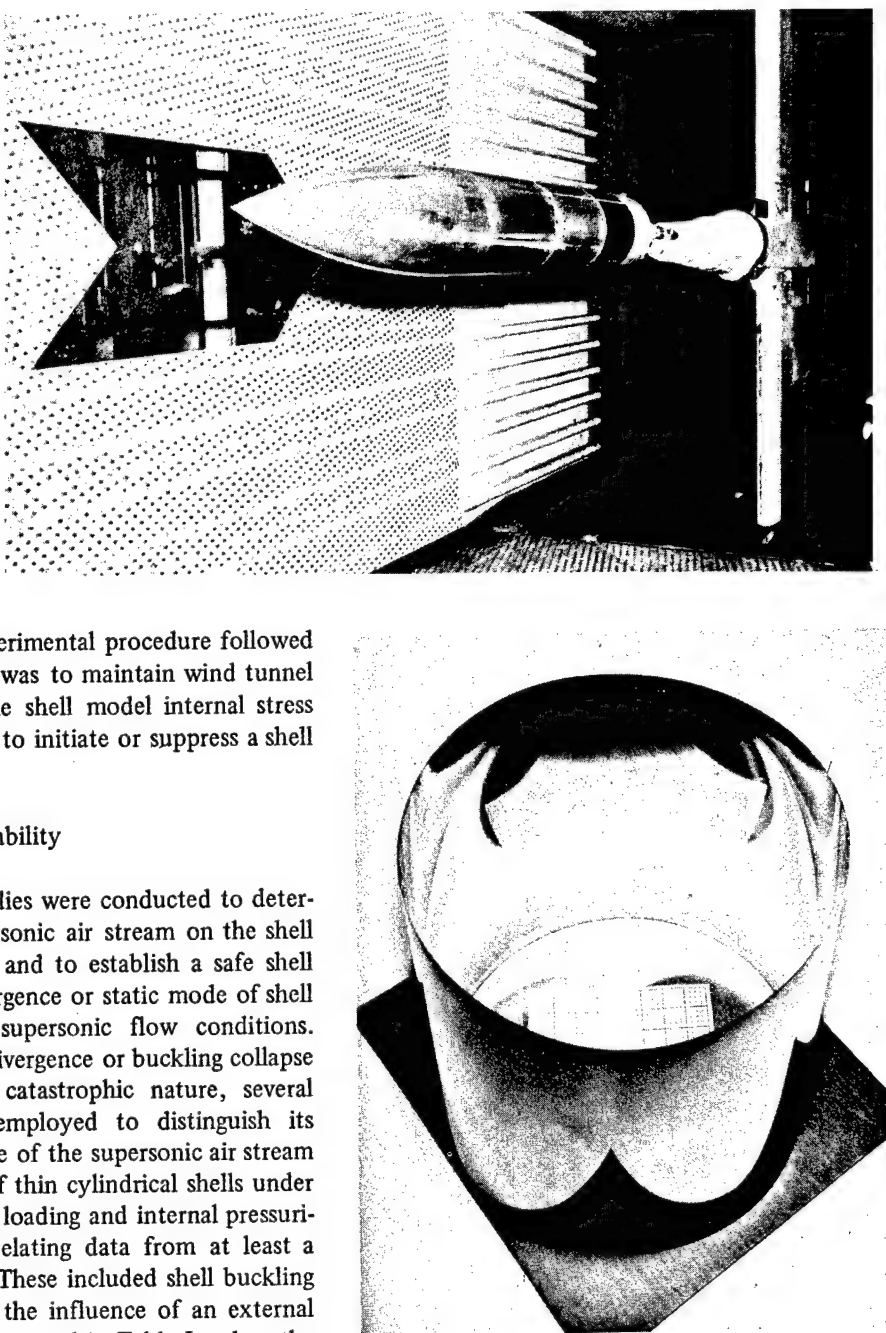


Fig. 9
Cylindrical Shell Flutter Model and Wind Tunnel
Installation

TABLE I BUCKLING INTERACTION AND FLUTTER DATA

Event	Source	M_∞	q	$R_e / t_1 \times 10^4$	$R_{1\infty}$ psf	No. times buckled	P lb.	\bar{p} psf	h in.	R/h	$\frac{\tilde{N}_x}{[3(1-\nu)]^{1/2}} \frac{\tilde{p}}{12(1-\nu)^{1/2}}$	$2qL/\beta D \times 10^{-4}$	$(q/\epsilon\beta)^{1/2} R/h$	Boundary layer	High speed movies	
Buckle	Ref. 4	3.0	425	2474	1	90	-0.037	0.0040	2000	0.056	-0.009	0.10	8.4	Laminar	—	
Buckle	Ref. 4	3.0	545	3173	1	700	3.93	0.0039	2050	0.458	1.03	0.14	9.4	Laminar	—	
Buckle	Ref. 4	0.0	—	—	—	390	0.0	0.0041	1950	0.230	0.0	—	—	Laminar	—	
Buckle	Ref. 4	0.0	—	—	—	350	0.0	0.0040	2000	0.218	0.0	—	—	Laminar	—	
Buckle	Ref. 4	0.0	—	—	—	400	0.0	0.0044	1820	0.205	0.0	—	—	Laminar	—	
Buckle	Ref. 4	0.0	—	—	—	0	-0.050	0.0040	2000	0.0	-0.012	—	—	Laminar	—	
Buckle	Jen. '68	2.6	308	126	1300	1	200	0.111	0.0033	2420	0.250	0.047	0.16	9.6	Turbulent	Yes
Buckle	Jen. '69	2.2	111	0.50	350	1	200	0.055	0.0032	2500	0.222	0.025	0.08	7.6	Laminar	Yes
Buckle	Jen. '66	0.0	—	—	—	2	130	0.900	0.0020	4000	0.406	1.03	—	—	—	—
Flutter	Ref. 5	1.2	1082	5.39	2600	0	0	0.240	0.0033	2420	0.0	0.100	2.01	22.6	Turbulent	—
Flutter	Ref. 5	1.2	1081	5.39	2600	0	0	0.270	0.0031	2580	0.0	0.128	2.43	24.0	Turbulent	Yes
Flutter	Ref. 5	1.5	858	4.33	2000	0	130	0.910	0.0021	3800	0.334	0.940	3.68	27.6	Turbulent	—
Flutter	Ref. 5	1.5	857	4.02	2000	0	105	0.480	0.0020	4000	0.298	0.548	4.25	29.0	Turbulent	Yes
Flutter	Ref. 5	1.2	1081	5.40	2600	0	210	0.520	0.0040	2000	0.169	0.148	1.13	18.6	Turbulent	Yes
Flutter	Jen. '69	2.2	313	1.47	1000	0	0	0.015	0.0032	2500	0.0	0.067	0.22	10.7	Turbulent	Yes
Flutter	Jen. '69	2.2	475	1.83	1500	0	0	0.060	0.0025	3220	0.0	0.045	0.44	15.8	Turbulent	—
Flutter	Jen. '68	2.2	102-	0.44-	322-	0	0	3.0-	0.0021	3880	0.0	0.91-	0.25-	11.5-13.3	Laminar	—
Flutter-Buckle	Jen. '69	2.2	313	1.47	1000	1	200	0.054	0.0032	2500	0.222	0.024	0.22	10.7	Turbulent	Yes

superimposed on Fig. 10 constitutes a reasonable design criterion for this observed static instability of the shell. The divergence or buckling mode shapes found in the presence of an air stream were also representative of those found in still air buckling studies. As an illustration the modal patterns were recorded in detail for the three data points singled out on the buckling interaction curve by the vertical arrows. Proceeding in the direction of increasing model internal pressure the modal patterns ranged from that of many long shallow elliptic type buckles equally spaced around the shell circumference for buckling under radial pressure only, to the classical diamond buckling pattern for combined axial loading and moderate internal pressure, to the fully axially symmetric bellows type mode for combined loads with high internal pressure levels [4].

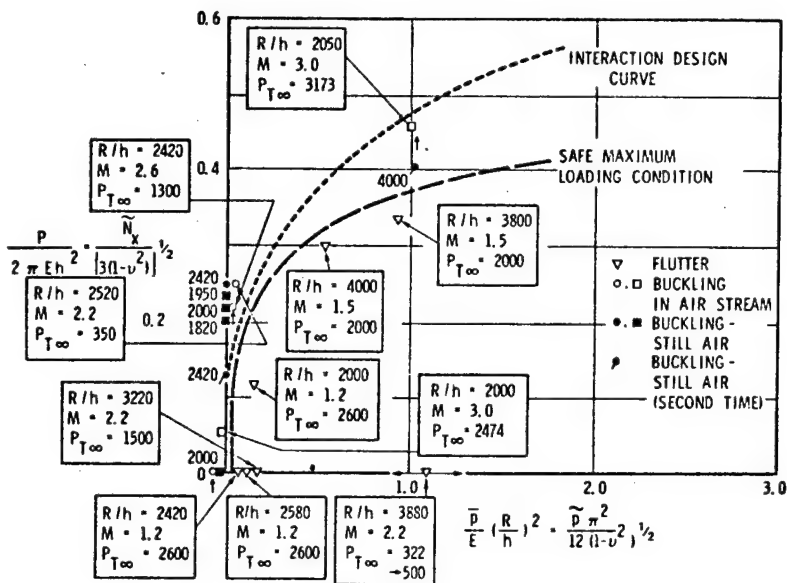


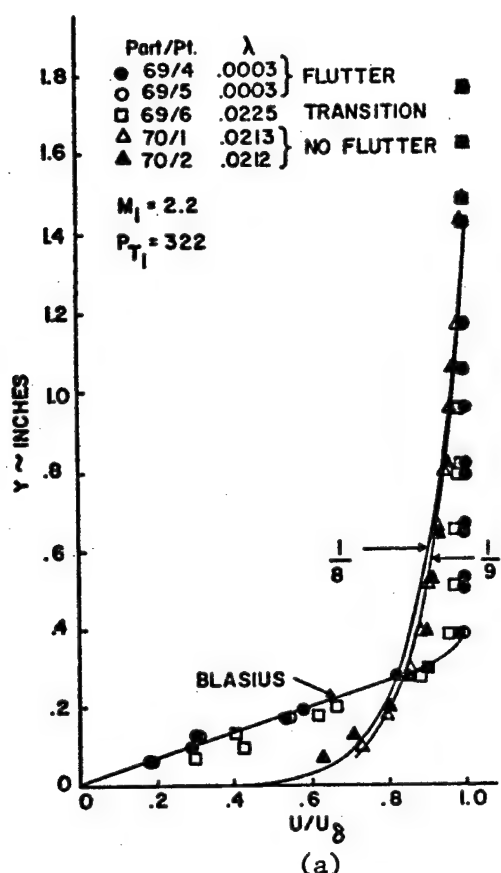
Fig. 10
Buckling Interaction Curves

On the basis of the experimental buckling interaction curve established in Fig. 10, a maximum safe loading condition was established that would guarantee a shell safe from buckling or diverging in a supersonic air stream when loaded under a combined internal pressure and axially compressive end loading. Although a cylindrical shell should be statically stable for all supersonic flow conditions when loaded under a combined stress state that lies below this curve it may still be dynamically unstable as indicated by the location of the open triangular symbols on this interaction curve.

It should be mentioned in passing, that the previously mentioned theoretical studies are in basic agreement with these experimental observations concerning the influence of a supersonic flow field on the classical buckling loads of cylindrical shells. Furthermore, the wind tunnel buckling studies were conducted under boundary layer profiles that ranged from laminar to fully developed turbulent. Nevertheless, no resulting viscous or fluid effects were observed on this static mode of shell instability.

Panel Flutter Instability

In addition to the static buckling instability described above, two types of dynamic instabilities were observed. One of these was a nondestructive limited amplitude fluttering motion whose maximum amplitude was on the order of four or five shell thicknesses. This motion was found to occur only in the presence of a laminar or near laminar profile of the type illustrated in Fig. 11a labeled Blasius. The amplitude time traces of two points on the shell surface during this motion are illustrated in Fig. 12 along with the model internal cavity pressure time history. Both the analogue and digitally plotted amplitude time histories are shown illustrating the harmonic character of the motion. The power spectral density, obtained from a fast Fourier transform of the digitized amplitude time history, are illustrated in Fig. 14a while the power spectral distribution is presented in Fig. 14b. The flutter mode appeared to be of a standing wave type with many waves around the circumference and one or two waves in the streamwise or shell axis direction as illustrated at the top of Fig. 15. For very small changes in the stress state of the shell or external flow conditions the amplitude time history would shift to the form illustrated in Fig. 13. Two modes of motion appear to be excited on the shell in this case as is illustrated by the power spectral density and distribution curves in Figs. 14c and d. Motion of the type illustrated in Figs. 12 and 13 were maintained on the shell for approximately one-half hour with no apparent damage to the structure. During this time a range of stress levels and



● PART NO. 81 TEST POINT NOS. 4, 5, 6 - VARIABLE RAKE
 □ PART NO. 81 TEST POINT NO. 6 - FIXED RAKE
 ▶ PART NO. 86 TEST POINT NO. 1 - FIXED RAKE
 $\delta^* = 0.292, \theta = 0.124$

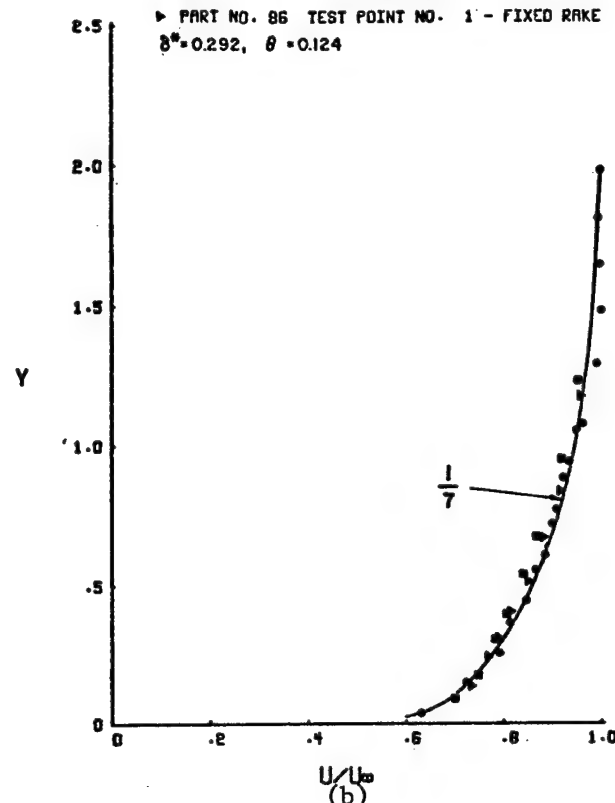


Fig. 11
 Illustration of Boundary Layer Profiles at Flutter Conditions

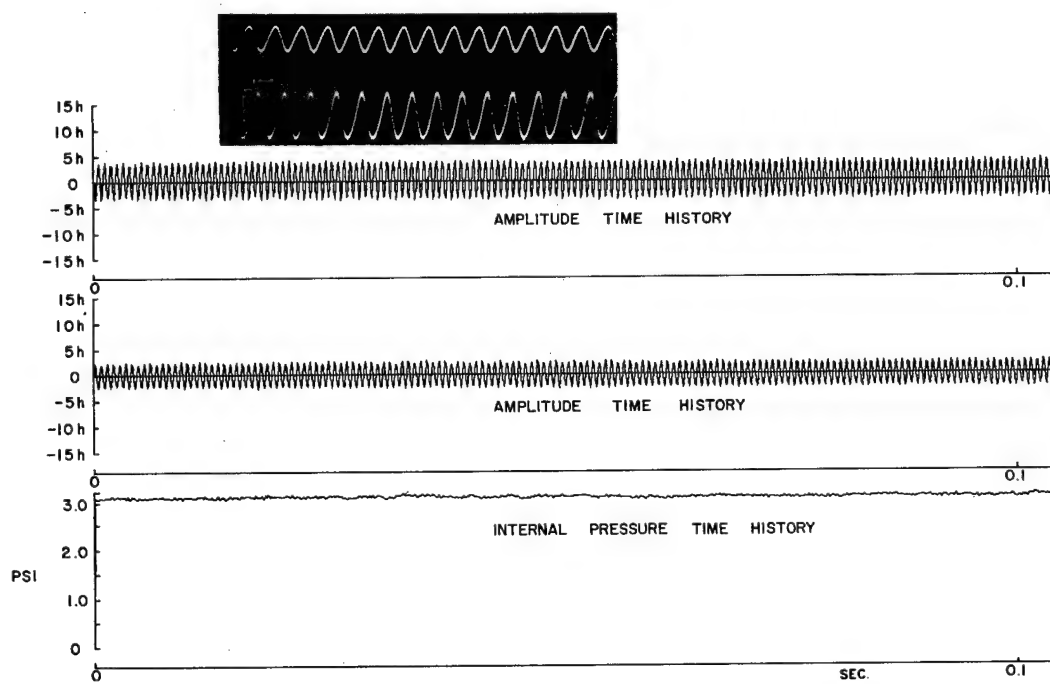


Fig. 12
 Amplitude Time and Internal Pressure Time Histories of Limited Amplitude Flutter

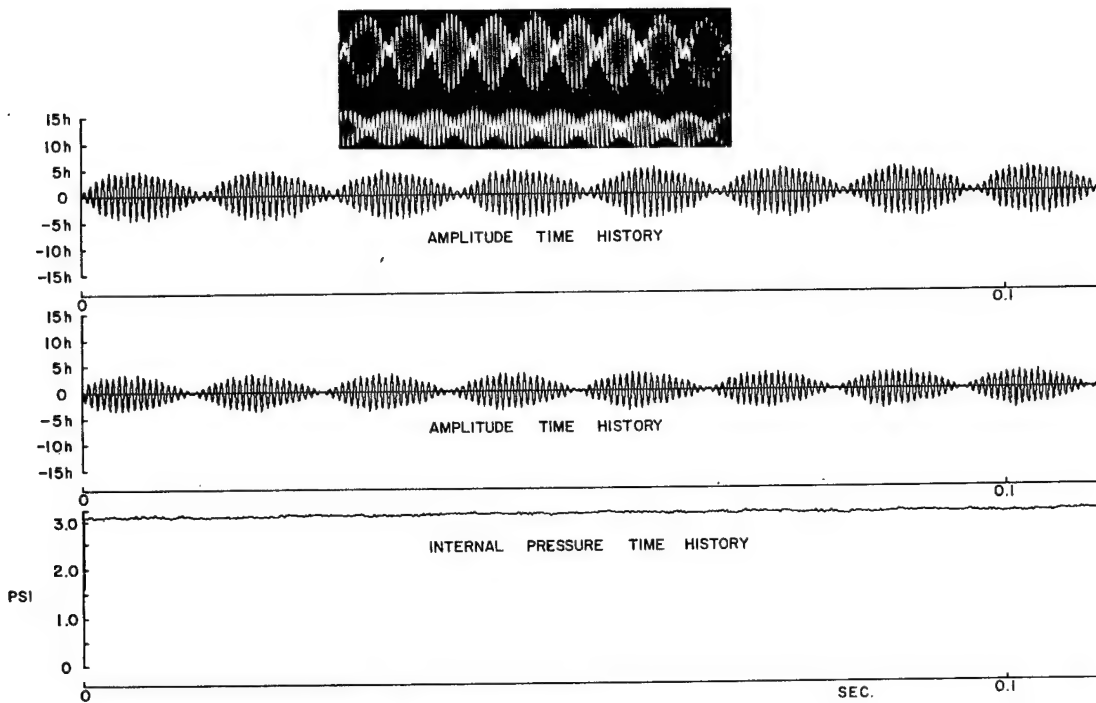
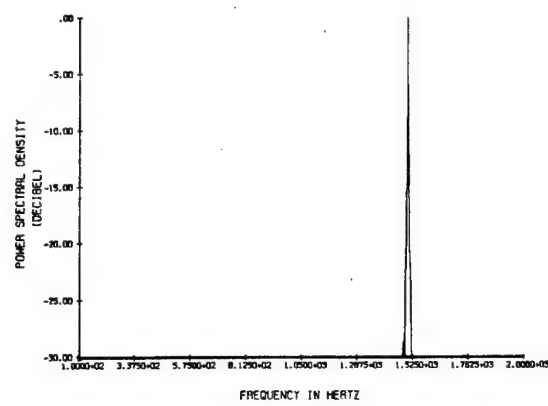


Fig. 13
Amplitude Time and Internal Pressure Time Histories of Limited Amplitude Flutter

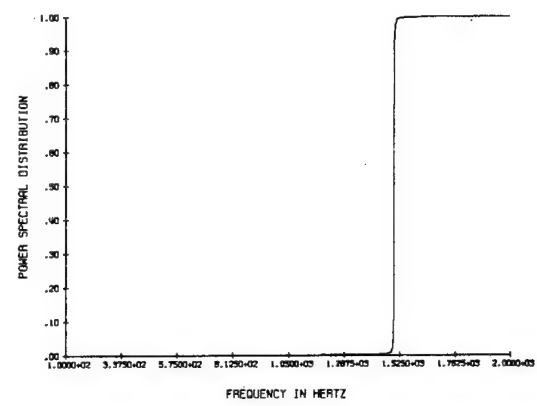
flow conditions were investigated as indicated by the two horizontal arrows associated with the triangular symbol of the buckling interaction curve of Figure 10. This limited amplitude flutter appears identical to that reported earlier in the literature. (11) (12) Further observations on this limited amplitude flutter instability have shown that for nearly perfect shells with minimal geometric imperfections the limited amplitude standing wave flutter mode may be transformed into a circumferentially traveling wave form also of limited amplitude motion whose front is nearly parallel to the airstream direction. (11) This is illustrated by the middle sketch of Figure 15. During the course of experiments on this type flutter it was also observed that this nondestructive limited amplitude flutter could be completely stabilized by tripping the laminar boundary layer making it turbulent and thicker as illustrated in Figure 11a. No limited amplitude motion of the above type was ever observed in the presence of a fully developed turbulent profile. (8), (15)

In contrast to this type of panel instability, a highly divergent flutter motion was also observed in the present study as illustrated by the amplitude and model cavity internal pressure time histories in Figure 16. These instabilities occurred in the presence of the fully developed turbulent profile shown in Figure 11b and were not observed in any of the prior experiments reported in the literature. Although the amplitude time traces of Figure 16 appear to be of limited amplitude, this actually represents a saturation of the instrumentation which was not designed to measure shell deformations on the order of an inch or so which occurred during this type of motion. In actuality, the highly divergent motion continues to grow until the shell is destroyed. This usually occurs within a few seconds at most. In this more catastrophic flutter, the power spectral density curves indicate a wider distribution of the energy in the frequency spectrum than that found for the limited amplitude flutter. This is attributed to the fact that the amplitude time traces are so highly divergent that some signal distortion is encountered in these traces due to the saturation of the instrumentation. In these cases the identification of the unstable flutter point in the frequency plane is better identified by the large jump in power illustrated by the power spectral distribution curves.

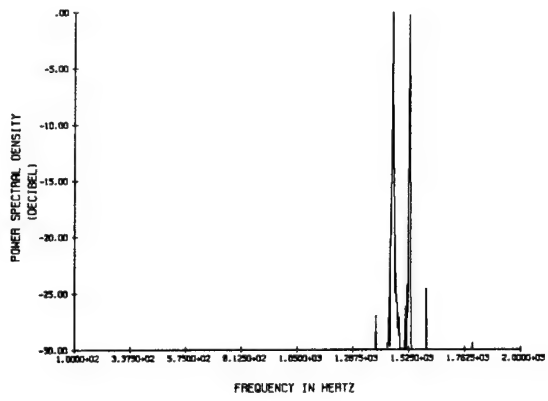
The highly divergent flutter mode shape was determined by viewing frames of several high speed movie film strips taken from different observations made on this instability. The characteristic wave form was found to be highly three dimensional, growing quite rapidly in amplitude as it propagated from the leading edge to the trailing edge of the shell. On the relatively thicker shells ($R/h - 2000-3000$) a series of wave fronts of the type illustrated by



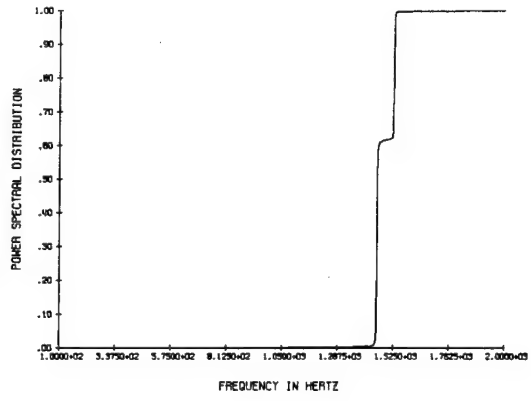
(a)



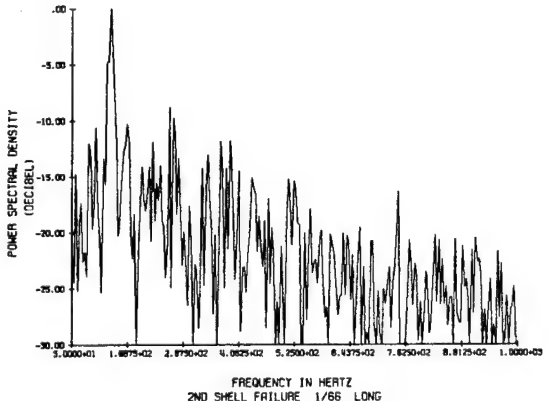
(b)



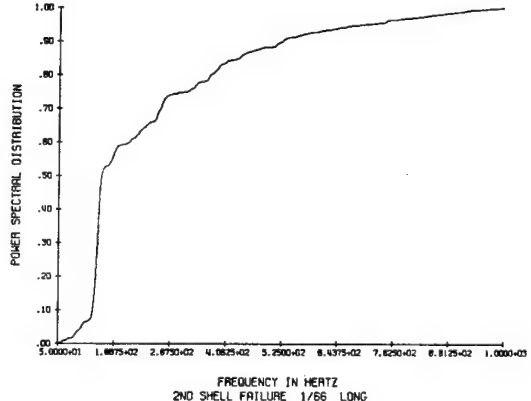
(c)



(d)



(e)



(f)

Fig. 14
Power Spectral Density and Power Spectral Distribution of Flutter Occurrences

the bottom sketch in Fig. 15 were observed to propagate rapidly from the leading edge to the trailing edge of the shell destroying it within a few seconds. The wave form was sharply defined being composed of two arms made up of small diamond buckles. The arms intersected to produce a 'V'-shaped wave front with the apex or lead buckle propagating along a shell generator in the airstream direction followed by the arms. The characteristic like arms appeared to maintain the same angular orientation relatively to the free stream velocity vector but grew in amplitude and length as they traveled downstream. In all cases, the arms of the wave front extended back to the shell leading edge as it propagated downstream; the leading edge acted as a local buckle source required for extending the length of the wave front. For the much thinner shells ($R/h \sim 4000$) a similar three-dimensional wave front was observed which, however, appeared more crescent-shaped in form than 'V' shaped. In addition, the wave front did not appear to be composed of small local dimples and did not appear to extend back to the leading edge of the shell. Some of the features of this wave form, however, were identical to those found on the thicker shells. That is, they were always highly divergent and a few series of the fronts would propagate over the shell destroying it within a second or so. The slightly different wave form found on the thinner shells was thought to be due to their small bending stiffness and more membrane-like character.

The basic experimental observations made during this phase of the experimental study indicate that the nature of the boundary layer is an important factor in the dynamical stability considerations of thin cylindrical shells exposed to a supersonic air stream. A laminar or nearly laminar boundary layer profile was found to induce panel flutter at much lower levels of free stream energy than did a turbulent profile. Panel flutter associated with the laminar boundary layer was limited in amplitude and its mode shape was of a standing or circumferentially traveling wave type whose characteristic length was on the order of the shell radius or length and whose amplitude was on the order of the shell thickness. When panel flutter was observed in the presence of a turbulent profile, however, it was always found to be catastrophic. In this latter case the flutter mode resembled a 'V' or wedge-shaped traveling wave front whose characteristic wavelength was small compared to the radius and length of the shell. The motion was highly divergent growing to many orders of magnitude greater than the shell thickness before destroying the shell.

CONCLUSIONS

As a result of this combined analytical and experimental investigation several definitive conclusions were reached concerning the influence of a supersonic flow field on the static and dynamic stability characteristics of thin cylindrical shell structures. The following are the more important conclusions obtained from this study.

Two basic types of instabilities were observed on thin cylindrical shell structures exposed to a supersonic flow field. A panel fluttering or dynamic instability was observed for certain combinations of stress states in the shell and external flow conditions. This instability could be quite catastrophic or nondestructive depending upon the nature of the fluid boundary layer over the shell. A divergence or buckling instability was also observed which appeared identical in every respect to the classical static buckling instability of thin cylindrical shells under combined axial compressive end loadings and/or internal pressure.

Although the present research illustrates that the external flow field does significantly complicate the dynamic stability features of the shell one simplifying observation was made. The classical still air buckling characteristics of a

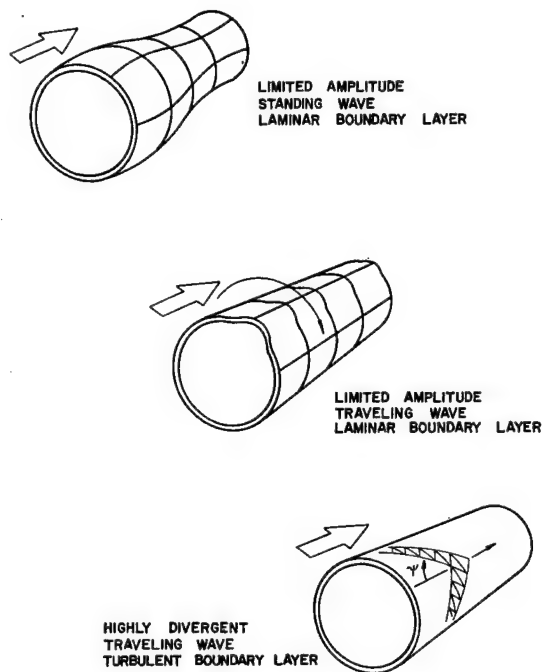
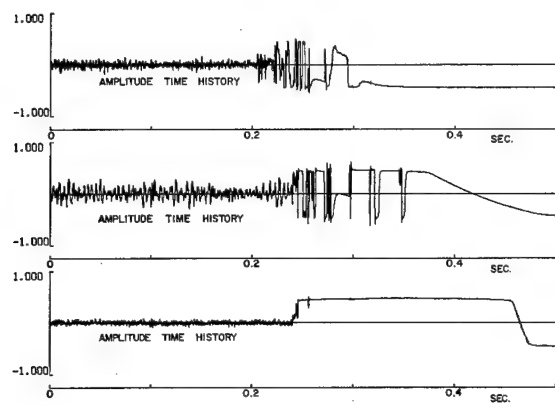
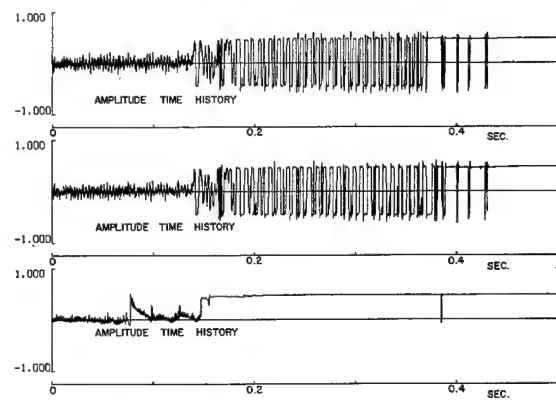


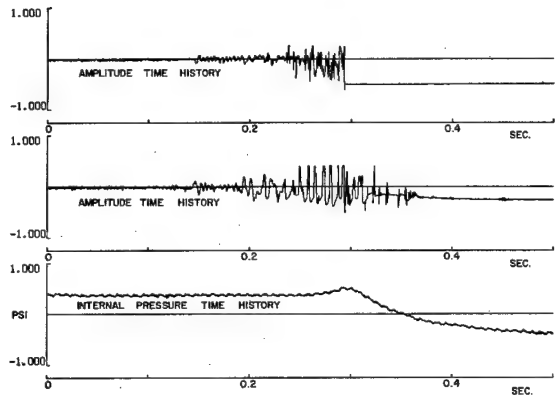
Fig. 15
Wave Form for Different Types of Flutter



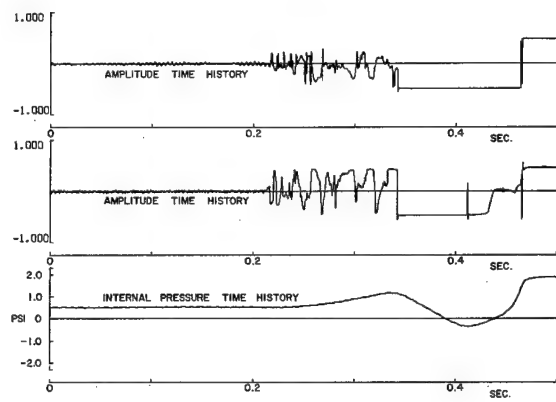
(a)



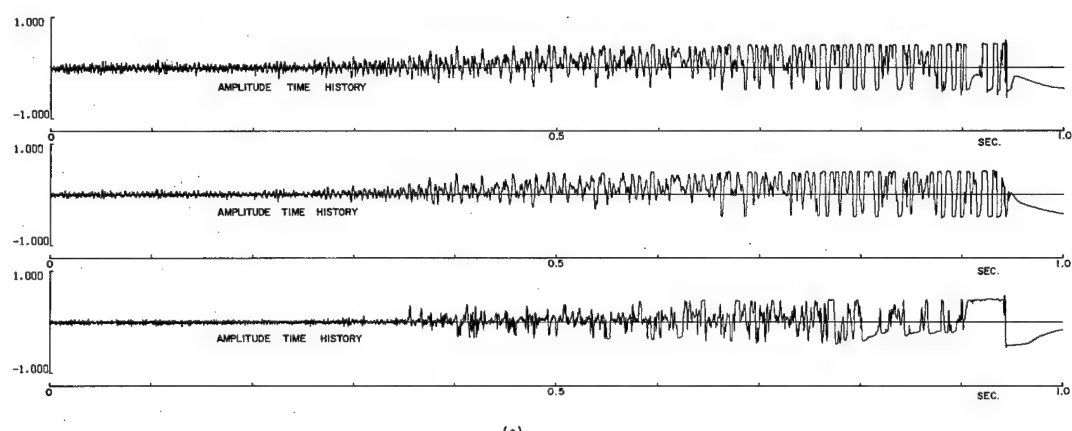
(b)



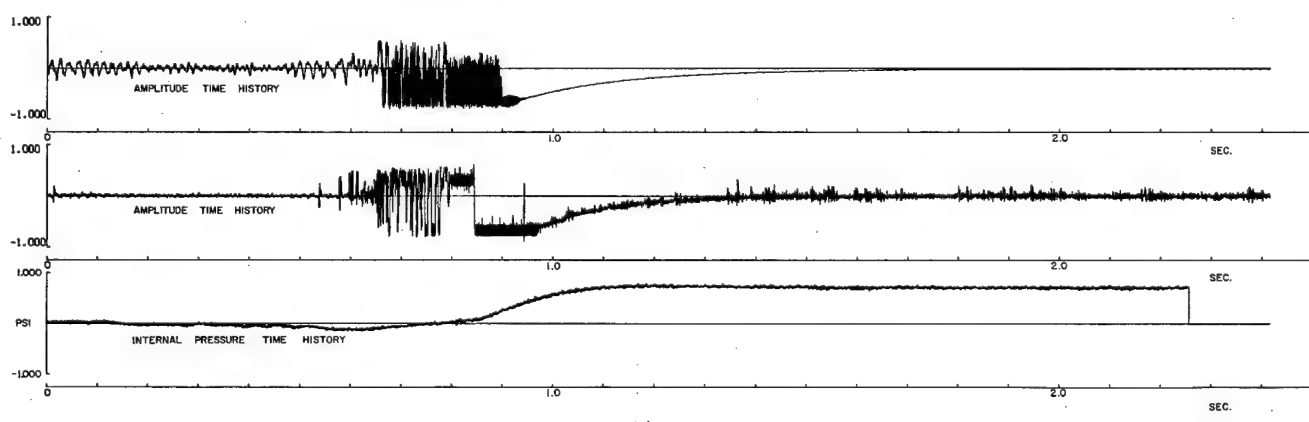
(c)



(d)



(e)



(f)

Figure 16. Amplitude-Time and Pressure-Time Histories of Highly Divergent Flutter

shell under combined internal pressure and axial compressive end loadings were not significantly influenced by the supersonic airstream. The wealth of available still air buckling data can consequently be employed to determine buckling loads of cylindrical shell structures under the above loading and external flow conditions.

The analytical results indicate that both the static and dynamic stability characteristics of the shell are strongly influenced by initial geometric imperfections that may exist in the shell surface due to fabrication techniques. It was readily demonstrated that stability margins (critical loads or airspeeds) could be easily reduced by a factor of two or more even though the initial imperfections were only on the order of one shell thickness.

Further analytical studies confirmed that the details in modeling of the structural boundary conditions were important when attempting to study the stability features of cylindrical shell structures exposed to an external flow field. Neglecting predeformation effects and investigating the stability of the shell structure about its unloaded geometric shape was found to underestimate its integrity against buckling or panel fluttering instabilities by as much as 25 percent in some cases. Predeformation effects, in general, were found to be stabilizing. Changes in only the in-plane structural boundary conditions of the shells were found to stabilize or destabilize the shell by an amount similar in magnitude to the predeformation effects.

One of the experimental observations indicated that the nature of the fluid boundary layer is an important factor to consider when investigating the panel flutter characteristics of the shell. A laminar or nearly laminar boundary layer profile will induce a panel flutter instability at much lower levels of free stream energy than will a turbulent profile. When panel flutter did occur in the presence of a turbulent profile, however, it was always found to be catastrophic; panel flutter instability in a laminar boundary layer was always a mild limited amplitude motion which caused no apparent damage to the structure even though it persisted for several minutes. The limited amplitude panel flutter could be suppressed, however, by tripping the boundary layer to a fully developed turbulent form.

All of the potential flow models employed in the analysis were found to be inadequate for predicting the panel flutter characteristics of the shells. While the modified piston theory approximation showed reasonably close correlation with the limited amplitude flutter instabilities for unstressed shells it was, in general, unconservative for the higher stressed shells. In addition, it did not correlate at all with the more highly divergent panel flutter instabilities. The slender body theory employed in the analysis did not predict even the qualitative features of the shell instability and was considered inadequate for the present study. In view of these findings, it is evident that the potential flow modeling is not adequate for predicting the shell's dynamic stability features. Viscous effects must be included in the description of the supersonic flow field. Unfortunately, this represents a significant complication to the analytical modeling of the problem.

Although the former analytical studies were conducted on the isotropic cylindrical shell, the results can, in certain cases, be extended to include ring and longeron stiffened cylindrical shells through the method outlined in [14].

NOTATION

a_∞	speed of sound in the freestream
B_0, B_1, B_2	matrices, dynamic stability problem
C_p	pressure coefficient
D	$Eh^3/12(1-\nu^2)$
E	elastic modulus
F	total stress function
h	shell thickness
k	$\omega R/U$, reduced frequency
L	shell length
M_∞	freestream Mach number
n	circumferential wave number
\bar{N}_x	applied axial stress resultant
\tilde{N}_x	$\bar{N}_x R [3(1-\nu^2)]^{1/2}/Eh^2$
$\tilde{N}_{x_{cr}}$	critical buckling load ratio
p	net radially outward loading per unit of shell surface area
p_a	amount of net radial shell loading due to aerodynamic pressure
\bar{p}	amount of net radial shell loading due to shell internal pressure
\tilde{p}	$(\bar{p}/E) (R/h)^2 [12(1-\nu^2)^{1/2}/\pi^2]$
p_∞	freestream static pressure
p_{t_∞}	freestream total pressure
q	freestream dynamic pressure
\tilde{q}	$(q/E) (R/h)^2$
R	shell radius
R_e	Reynold's number
T_∞	freestream static temperature
T_{t_∞}	freestream total temperature
U	freestream velocity
u, v, w	shell displacement components; axial, circumferential and radial respectively
U_δ	velocity at outer edge of boundary layer
\bar{w}_i	initial imperfection
\hat{w}	total deformed mode shape with respect to initially perfect cylinder
x, y, z	coordinate axes
Z_m	$m\pi/(L/R)$
α	x/R
β	$[M^2 \cdot 1]^{1/2}$
λ	$2qL^3/\beta D$, aerodynamic loading parameter
μ	$\rho_s h/\rho_\infty R$, mass ratio parameter

$\tilde{\mu}$	imperfection amplitude ratio normalized against shell thickness
ν	Poisson's ratio
ρ_∞	freestream mass density
ρ_s	shell mass density
τ	U_t/R
ϕ	perturbation velocity potential
$\nabla^4(\)$	$[(\),_{xx} + (\),_{yy}]^2$
ω	frequency of motion

BIBLIOGRAPHY

1. Almroth, B.O., "Influence of Imperfections and Edge Restraint on the Buckling of Axially Compressed Cylinders," NASA CR-432, Apr. 1966.
2. Barr, G.W., "The Influence of Initial Imperfections and Edge Constraint on the Buckling and Aeroelastic Stability of Cylindrical Shells," Ph.D. Thesis, July 1967, University of Kansas.
3. Barr, G.W., and Stearman, R.O., "Aeroelastic Stability Characteristics of Cylindrical Shells Considering Imperfections and Edge Constraint," *AIAA Journal*, Vol. 7, No. 5, May 1969, pp. 912-919.
4. Barr, G.W., and Stearman, R.O., "The Influence of a Supersonic Flow Field on the Elastic Stability of Thin Cylindrical Shells," *AIAA Journal*, Vol. 8, No. 6, June 1970, pp. 993-1000.
5. Carter, L.L., and Stearman, R.O., "A Theoretical Investigation of the Aeroelastic Stability of Isotropic Cylindrical Shells at Both the High and Low Supersonic Mach Numbers," AFOSR Final Technical Report TR 66-1930, Oct. 1966.
6. Dowell, E.H., and Widnall, S.E., "Generalized Aerodynamic Forces on an Oscillating Cylinder," *Quart. Appl. Math.*, Vol. 24, Apr. 1966, pp. 1-17.
7. Franklin, J.N., "On the Numerical Solution of Characteristic Equations in Flutter Analysis," *Journal Assoc. Comp. Mach.*, Vol. 5, 1958, pp. 45-51.
8. Horn, W.J., et al., "Recent Contributions to Experiments on Cylindrical Shell Panel Flutter," AIAA/ASME 12th Structures, Structural Dynamics and Materials Conference, Anaheim, California, Apr. 19-21, 1971.
9. Krumhaar, H., "The Accuracy of Applying Linear Piston Theory to Cylindrical Shells," *AIAA Journal*, Vol. 1, No. 6, June 1963, pp. 1448-1449.
10. Miles, J.W., "Supersonic Flutter of a Cylindrical Shell, Part I," *Journal of Aero. Science*, Vol. 24, No. 2, Feb. 1957.
11. Olson, M.D., "Supersonic Flutter of Circular Cylindrical Shells Subjected to Internal Pressure and Axial Compressions," GALCIT Structural Dynamics Report SM 65-7, AFOSR 65-0599, Apr. 1965. See also *AIAA Journal*, Oct. 1967, pp. 1849-1856, and May 1966, pp. 858-864.
12. Stearman, R.O., Lock, M.H., and Fung, Y.C., "AMES Tests on the Flutter of Cylindrical Shells," GALCIT Structural Dynamics Report SM 62-37, Dec. 1962.
13. Stearman, R.O., "Research on Panel Flutter of Cylindrical Shells," AFOSR Final Scientific Report 64-0074, Jan. 1964.
14. Stearman, R.O., "Flutter of a Ring of Panels," *AIAA Journal*, Vol. 2, No. 8, Aug. 1964, pp. 1441-1448.
15. Stearman, R.O., "An Experimental Study on the Aeroelastic Stability of Thin Cylindrical Shells at the Lower Supersonic Mach Numbers," Final Technical Report AFOSR 66-2828 and ARL 67-0006, Dec. 1966.
16. *Test Facilities Handbook*, 6th ed., Arnold Engineering Development Center, Air Force Systems Command, United States Air Force, Nov. 1966.
17. Weingarten, V.I., et al., "Final Report on Development of Design Criteria for Elastic Stability of Thin Shell Structures," STL/TR-60-0000-19425, Dec. 31, 1960, Space Technology, Inc.